Decentralized Relay Selection Schemes in Uniformly Distributed Wireless Sensor Networks

Farrokh Etezadi, Keyvan Zarifi, Ali Ghrayeb, and Sofiène Affes

***Abstract*—We study three relay selection schemes for uniformly distributed wireless sensor networks: 1) optimal selection where the relays that maximize the signal-to-noise ratio (SNR) at the destination are selected, 2) geometry-based, which is based on selecting the closest nodes to the source, and 3) random selection in which the nodes are selected randomly from a certain neighborhood of the source. In all schemes, we assume that all relays operate in the amplify-and-forward mode and transmit with equal average powers and each relay has only access to its backward channel and location. For each relay selection strategy, we propose a decentralized protocol whereby proper nodes choose to act as relays without requiring any central coordinating entity or any inter-node information transfer. We derive expressions for the average SNR at the relays and destination while assuming that the source-node distances and the inter-terminal channel links are completely random. We show that, for all proposed schemes, the SNR variance at the destination converges to zero as the number of relays increases. While each selection scheme has its pros and cons, we derive a sufficient condition under which the average SNR at the destination becomes independent of the selection scheme employed.**

***Index Terms*—Amplify-and-forward, cooperative communications, relay selection, wireless sensor networks.**

I. Introduction

It is now well-understood that cooperative single-antenna terminals can effectively emulate centralized multiple transmit antenna systems to increase the link reliability, transmission coverage, spectral efficiency, or a combination thereof. A practically important form of inter-terminal cooperation is the case when possibly multiple intermediate terminals act as relays to convey a source signal to its intended destination. When a surplus of relaying candidates are at disposal, a proper choice of relaying terminals can substantially improve the efficiency of the cooperative network and the target performance metric at the destination. This has motivated extensive research efforts in developing a variety of relay selection techniques. An intuitive relay selection scheme is to choose a single terminal that is deemed most appropriate with respect to some objective function such as minimizing the channel outage probability [1]- [6]. This minimalist approach to the use of relays is theoretically well-justified in some scenarios. For instance, it has been shown in [5] that if the single optimal terminal is selected as the relay, the achieved spatial diversity order is equal to the case when all available candidates act as relays. Despite the above fact, practical concerns sometimes discourage putting the onus on only one terminal to establish a reliable connection between the source and the destination. A prime example is the case when a source in a wireless sensor network (WSN) with battery-powered nodes aims to transmit to a distant destination, but requires some cooperation from its neighboring nodes due to its limited battery or insufficient maximal transmit power. As the nodes' battery replacement is often impractical if not impossible, using only one node as a relay results in an early exhaustion of the relay's limited energy resource, and consequently leads to a considerable reduction in the network lifetime. In contrast, using multiple relays not only can improve the spatial diversity order under fairly general assumptions, it also can substantially increase the network longevity when the nodes operate under a total transmission power constraint. Under such constraint, each relaying node decreases its transmission power proportional to the number of selected relays. This guarantees, on average, less power transmission from every node and more even power dissipation among all nodes, and, hence, a substantially prolonged network lifetime.

A number of efficient multi-relay cooperative schemes have been developed in the literature [7]- [16]. In [7], channel outage probability expressions are derived for several multi-relay decode-and-forward (DF) cooperative schemes in which the relays decode the source signal and either resend it through orthogonal channels or use a space-time code (STC) to concurrently retransmit it using a single channel. While the STC-based cooperative scheme is more spectrally efficient than its repetition-based counterpart, it entails a higher relays' coordination and system complexity. A cooperative communication scheme is developed in [8] where multiple terminals use an amplify-and-forward (AF) technique to relay the signal to the destination via orthogonal channels. Assuming that the SNRs corresponding to all channels from the relays to the destination are statistically independent, the average symbol error rate expression is derived in [8] and it is proved that the cooperative system enjoys the full spatial diversity order. A similar assumption as in [8] is used in [9] to derive the channel outage probability expression and obtain the optimal relays' power allocation in a multi-relay AF cooperative scheme. Assuming that the forward channels are available at the

Manuscript received July 20, 2010; revised December 19, 2010 and August 18, 2011; accepted October 24, 2011. The editor coordinating the review of this paper and approving it for publication was C. Tellambura.

This paper was made possible in part by NPRP grant #08-055-2-011 from the Qatar National Research Fund (a member of Qatar Foundation).

F. Etezadi is with the University of Toronto, Toronto, ON, Canada (e-mail: fetezadi@comm.utoronto.ca).

K. Zarifi is with Huawei Technologies, Kanata, ON, Canada (e-mail: zarifi@ieee.org).

A. Ghrayeb is with Concordia University, Montreal, QC, Canada (e-mail: aghrayeb@ece.concordia.ca).

S. Affes is with the Institut National de la Recherche Scientifique-Énergie, Matériaux, et Télécommunications (INRS-EMT), Université du Québec, Montreal, QC, Canada (e-mail: affes@emt.inrs.ca).

Digital Object Identifier 10.1109/TWC.2012.010312.101314

relays, [10] proposes a cooperative beamforming technique using the set of relays that have successfully decoded the source signal. Computationally affordable SNR suboptimal multi-relay selection schemes are proposed [11] and efficient relay subset selection techniques in cooperative networks with partial DF transmission are developed in [12]. In [13], the authors consider relay assignment schemes for large multiple-pair networks. Each selected relay uses network coding and serves only one pair of nodes. It is shown that all nodes achieve the full spatial diversity which is the number of available relays. Other contributions on power allocation and relay selection in multi-relay cooperative networks can be found, for instance, in [14]-[16].

Most of the current literature on relay selection techniques either completely ignore or only implicitly take into account the effect of the network topology and the terminals distribution on the performance of cooperative systems. Often, the only considered factor that is related to the network topology is the inter-terminal (such as the source-relay) distance effect that manifests itself in the signal path-loss. When the latter effect is taken into account, the impact of the signal path-loss and the small-scale fading is usually lumped together and is jointly shown by a single random channel coefficient whose fixed second-order moment is proportional to the path-loss and whose different realizations represent the randomness of the small-scale fading. Such a simplistic approach to model the effects of the network topology and the terminals distribution may not always be appropriate due to at least the following two reasons: 1) This model may not sufficiently explain the effects of the network-descriptive parameters such as the network size, the terminals distribution, and the terminals density on the performance of cooperative systems; and 2) this model does not offer any analytical description of the inter-terminal distances, and, consequently, the signal path-losses. Therefore, it may not facilitate obtaining analytical results on the performance of the cooperative schemes that select the relays based on their geographical locations.

The main motivation of this work is the limited available research results on relay selection techniques that explicitly take into consideration the network's topological structure. We contribute in this thrust of research by introducing energy-fair decentralized relay selection techniques in WSNs whose nodes are uniformly distributed according to a two-dimensional homogeneous Poisson process [17]-[19]. The uniform distribution is probably the most reasonable model to describe the network's structure when there is no apriori knowledge of the nodes' locations. It can also accurately describe the topology of WSNs whose nodes could move randomly and without any coordination with one another.

We assume that the source and all relaying candidates are the WSN nodes. We consider a two-phase AF cooperative scheme where in the first phase the source broadcasts its signal and in the second phase K nodes act as relays by amplifying their received signals and resending them to a distant destination through dedicated channels. We use the simple AF scheme as it does not require the nodes to perform the complicated signal decoding and re-encoding procedure. Considering the practical case where the nodes are only aware of their own backward channel as well as their own locations, we develop three decentralized competition-based relay selection techniques in which the nodes use their own locally-available information to compete with one another and acquire the relaying status. First, the optimal relay selection technique is proposed where the K nodes with the highest SNRs win the competition and act as relays. Among all those techniques that do not use any information of the nodes' forward channels to select the proper set of relays, this approach can provide the highest SNR at the destination. Despite being SNR-optimal, such an approach is shown to be excessively energy wasteful. Exploiting the fact that the changes in the network topology can have a much slower dynamic than those in the terminals' backward channels, we develop a substantially more energy-efficient alternative technique upon which closest K nodes to the source acquire the relaying status. In addition to its energy efficiency, it is shown that the latter technique results in an average SNR performance at the destination that, in most cases, is only a fraction of a dB less than that of its optimal relay selection counterpart. In spite of its clear advantages, the above geometry-based relay selection approach may over-exploit the nodes that are closer to the source especially when the network topology is static. This motivates us to propose a third relay selection scheme wherein a periodically-renewed set of K nodes from a certain neighborhood of the source act as relays. This random relay selection scheme is shown to be both energy efficient and fair towards all nodes at the expense of a possible SNR drop at the destination.

Taking into account the facts that all source-node distances and all inter-terminal channel links are random quantities, we analytically study the performance of the proposed relay selection techniques. First, the cumulative distribution function (CDF) of the k-th largest SNR at the nodes is derived and is used to obtain the average SNR at the k-th relay in the optimal relay selection technique. Then, the probability density function (PDF) of the k-th closest node to the source and a randomly-selected node from an R-neighborhood of the source are used to obtain the average SNR at the k-th selected relay in the geometry-based and in the random relay selection schemes, respectively. When the relays are randomly selected, the choice of R, the radius of the relay-selection neighborhood around the source, can have a significant effect on the performance of the cooperative system. Therefore, a technique to determine the optimal R is proposed by minimizing a properly-defined outage event.

The average SNR expression at the destination is also obtained and a sufficient condition is derived under which the latter expression becomes independent from the approach used to select the relays. This condition has a particular practical importance as it clarifies when the fair and energy-efficient random relay selection technique can be used without degrading the signal reception quality at the destination. When the random relay selection technique is used, it is proven that the average SNR at the destination is an increasing function of the number of selected relays. As the randomly-selected relays operate under a total average transmission power constraint, increasing the number of relays implies a decrease in each relay's average transmission power and, hence, an improvement in the network lifetime. Finally, the SNR variance at the destination is analytically studied and

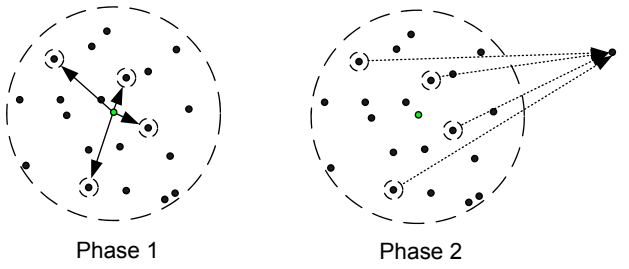

Fig. 1. The two-phase collaboration system description.

is shown to converge to zero in all schemes as K increases. This verifies that when there is a large number of relays, all the results that hold for the average SNR at the destination also apply to the instantaneous SNR with high accuracy.

The rest of this paper is organized as follows. Section II describes the system and signal models. Section III introduces the proposed relay selection schemes. Section IV analyzes the SNR averages and variances for all relay selection schemes. Simulation results are presented in Section V. Concluding remarks are given in Section VI.

II. System Description

Consider a large WSN wherein identical sensor nodes are uniformly distributed according to a two-dimensional homogeneous Poisson process with intensity ρ [17]-[19]. Assume that a node s aims to transmit to a distant destination located outside the WSN using a two-phase AF cooperative transmission protocol shown in Fig. 1 and described as follows. In the first phase, s transmits its signal and all other nodes within its transmission range receive a noisy and attenuated version of the transmitted signal. In the second phase, K receiver nodes switch from the listening mode to the transmission mode, amplify their received signal and retransmit it to the destination through orthogonal channels and under an average total transmission power constraint. The strategy to determine the relaying nodes and the technique to administer the orthogonal transmissions among the relays will be presented in Section III. The above cooperative communication protocol is implemented in a pragmatic, unsupervised environment in which there is no channel state information at the source and no synchronization or information exchange among the relays and no channel feedback from the destination to the nodes. We assume that the node k has only knowledge of $D_{s,k}$, its distance to s, along with $h_{s,k}$, the fading coefficient of the link between s and k, and periodically transmits this information to the destination. In addition to the instantaneous channel state and distance information sent from the relays, the destination has also knowledge of D, its distance from the network, as well as $h_{k,d},\ k = 1, \ldots, K$, the fading coefficients of the links from the relays to the destination. Note that the destination is assumed to be in a far-field, and, as such, its distance from every node on the network can be well-approximated by D. Noise at all terminals is zero-mean white Gaussian with variance σ^2, and all inter-terminal small-scale fadings can be modeled by independent zero-mean Gaussian random variables with a variance of $1/2$ per dimension.

The received signal at the relaying nodes in the first phase can be represented as

$$y_k = \sqrt{p_s} h_{s,k} D_{s,k}^{-\nu/2} x + n_k \qquad k = 1, \ldots, K \tag{1}$$

where p_s is the transmission power from s, $\nu \in [2, 6)$ is the path-loss exponent, x is the zero-mean unit-variance data transmitted from s, and $n_k \sim \mathcal{CN}(0, \sigma^2)$ is the additive white Gaussian noise. We adopt the common assumption that there is a relay-free zone of unit distance around the source [20], [21] to avoid the problem of the received power divergence in the close vicinity of the source. The signal transmitted from s is solely intended to reach the potential relays in a neighborhood of the source. As such, p_s is selected small enough to avoid inflicting a considerable interference on farther nodes of the network. From (1), the SNR at node k can be expressed as

$$\gamma_k = \varsigma |h_{s,k}|^2 D_{s,k}^{-\nu}, \tag{2}$$

where $\varsigma \triangleq p_s/\sigma^2$ and the average SNR is given by $\bar{\gamma}_k = \varsigma \cdot \mathrm{E}\left\{|h_{s,k}|^2 D_{s,k}^{-\nu}\right\}$. Note that the randomness of $D_{s,k}$ is due to the uniform distribution of the nodes on a two-dimensional plane. Throughout the paper, it is assumed that all channel coefficients, distances between the source and relays, the terminals' noises, and the transmitted signal from the source are r.v.s. The statistical expectations are always taken with respect to the joint distribution of all r.v.s inside their arguments.

The received signal from the k-th relay at the destination can be represented as

$$y_d^{[k]} = \sqrt{\beta_k} h_{k,d} D^{-\nu/2} y_k + n_d^{[k]} \qquad k = 1, \ldots, K \tag{3}$$

where $n_d^{[k]}$ is the background noise corrupting the received signal from the k-th relay and

$$\beta_k \triangleq \frac{1}{K} \cdot \frac{P_T}{\mathrm{E}\{|y_k|^2\}} = \frac{1}{K} \cdot \frac{P_T}{\sigma^2(\bar{\gamma}_k + 1)} \qquad k = 1, \ldots, K \tag{4}$$

is the normalization factor at the k-th relay. It directly follows from (4) that the instantaneous transmission power from the k-th relay is $\xi_k = \beta_k |y_k|^2 = (P_T/K) \cdot (|y_k|^2 / \mathrm{E}\{|y_k|^2\})$. As such, regardless of which set of K nodes act as relays, the average transmission power from every relay is fixed and is given by $\mathrm{E}\{\xi_k\} = P_T/K, k = 1, \ldots, K$. This property guarantees an equitable power dissipation from the selected relays and, consequently, prolonging the network lifetime by avoiding over-exploiting some of the selected relays. Moreover, the average of the total transmission power from the whole network during the relaying phase is always equal to P_T. This makes it possible to fairly compare the performances of different relay selection schemes.

Assume that the destination uses optimal maximum ratio combining (MRC) to estimate x from the set of signals received from the relaying nodes. Using (1) and (3) and after some manipulation, it can be shown that the soft symbol estimate at the MRC receiver output is given by

$$y_d = \sum_{k=1}^{K} \frac{\sqrt{p_s \alpha_k} h_{s,k}^* h_{k,d}^* D_{s,k}^{-\nu/2}}{\sigma^2 \left(1 + \alpha_k |h_{k,d}|^2\right)} \cdot y_d^{[k]} \tag{5}$$

where

$$\alpha_k \triangleq \beta_k D^{-\nu} = \frac{1}{K} \cdot \frac{P_T}{\sigma^2 D^{\nu}} \cdot \frac{1}{\bar{\gamma}_k + 1} \tag{6}$$

and * is the conjugate operation. It follows from (3) and (5) that the resulting SNR at the destination is

$$\gamma_d = \sum_{k=1}^{K} \theta_k \tag{7}$$

where

$$\theta_k \triangleq \frac{\alpha_k |h_{k,d}|^2}{1 + \alpha_k |h_{k,d}|^2} \cdot \gamma_k = \frac{\alpha_k |h_{k,d}|^2}{1 + \alpha_k |h_{k,d}|^2} \cdot \frac{\varsigma |h_{s,k}|^2}{D_{s,k}^{\nu}}. \tag{8}$$

III. Relay Selection Schemes

It remains to develop strategies upon which K nodes choose to switch to the transmission mode and relay a scaled version of their received signal from s to the destination through orthogonal channels. These strategies should be applicable in a decentralized WSN wherein there is no central coordinating or processing unit and no synchronization or information exchange among the nodes or knowledge about $h_{k,d}$, $k = 1, \ldots, K$ at the nodes.

1) Optimal Relay Selection: Aiming to maximize γ_d, it immediately follows from (7) that the best relaying set is the set of K nodes with the K largest θ_k. Unfortunately, as θ_k depends on $h_{k,d}$, it is unknown at node k and therefore it cannot be directly adopted as a measure to select the relays. However, as can be observed from (8), θ_k is an increasing function of γ_k, which itself is directly proportional to $|h_{s,k}|^2 D_{s,k}^{-\nu}$ that is known at node k. The above discussion suggests that, being unaware of $h_{k,d}$, the optimal relaying set is the set of K nodes with the largest γ_k. Selecting the K nodes with the largest SNRs is also intuitively correct: Since the nodes are completely oblivious to the forward hop, they can make decision based only on the backward hop. Hence, the optimal relays are the ones that have the best signal reception quality. In what follows, we show how the K nodes with the largest γ_k may choose to act as relays and transmit through orthogonal channels.

First, a clear-to-send (CTS) flag from the destination triggers each node k to start its down-counter from the initial value of[1]

$$T_k^{(o)} = \frac{\lambda^{(o)} D_{s,k}^{\nu}}{|h_{s,k}|^2} \tag{9}$$

where $\lambda^{(o)}$ is a scalar. As the distance between the destination and every node can be considered equal to D, all nodes receive the CTS signal simultaneously and therefore the k-th counter that expires to zero belongs to the node with the k-th smallest $D_{s,k}^{\nu}/|h_{s,k}|^2$, or, equivalently, the k-th largest γ_k. Once the first counter expires, the corresponding node switches to the transmission mode and acts as the first relay by forwarding its signal to the destination. As soon as the relayed signal is overheard by other nodes, they pause their down-counters until the channel clears. At the end of the first relay transmission period, this relay switches back to the listening mode and sets its counter to its initial value while all other nodes resume their countdown until the next counter expires to zero. Then, the node with the expired counter acts as the second relay and all remaining nodes pause their counters again until the relay ends its transmission. Similar to the first relay's transmission procedure, the second relay switches back to the listening mode and resets its counter to (9) at the end of its transmission while the remaining nodes (other than the first and the second relays) continue again their countdown. This procedure continues until the total number of the relayed signals reaches K. Then, every node that has not acquired the relaying status resets its counter to its initial value and waits in the listening mode for another round of source transmission and relaying competition. It should be mentioned that the countdown pauses are necessary to avoid collision among the relays' transmitted signals as, otherwise, it is possible that some nodes expire their counters and relay their signals during an ongoing relay transmission.

As the channel fading coefficients $h_{s,k}$ may vary frequently, the set of nodes with the K largest SNRs may change substantially from one source transmission frame to the next one. This fact suggests that, in this scheme, all nodes are viable candidates to achieve the relaying status, and, therefore, should always switch between the listening and the transmission modes without having the privilege to leave to the sleeping mode and preserve energy. Note that the energy consumption of a typical transceiver in the listening mode is up to three orders of magnitude larger than its energy consumption in the sleeping mode where both receive and transmit circuitries are switched off [23]. This can be excessively energy wasteful especially in scenarios where K is a small fraction of the total number of nodes within the transmission range of s. The above practical drawback of the optimal relay selection scheme motivates us to propose the following alternative.

2) Geometry-based Relay Selection: As the network topology is fixed or changes very slowly in many WSN applications, the rate of changes in $D_{s,k}$ is typically much less than the rate of changes in $h_{s,k}$. This property, along with the fact that γ_k is inversely proportional to $D_{s,k}^{\nu}$, can be exploited to properly modify the aforementioned relay selection policy such that a substantial amount of network energy is preserved at the expense of a small degradation in the signal reception quality at the destination. Assume that the initial values of nodes' counters are set to

$$T_k^{(g)} = \lambda^{(g)} D_{s,k}, \tag{10}$$

where $\lambda^{(g)}$ is a scalar. Once the network receives the CTS signal, exactly the same procedure as in the optimal relay selection scheme starts until the K-th relay forwards its signal. The only difference is that as soon as the K-th relay's transmission ends, all the nodes that have not acquired the relaying status switch to the sleeping mode for $T^{(g)}$ seconds. $T^{(g)}$ depends on the prior knowledge about the expected rate of changes in the network topology and may be chosen in the order of the time required for the transmission of several hundred data frames. In fact, IEEE 802.15.4 standard permits nodes to be left in the sleeping mode for more than 99% of the time [25]. After $T^{(g)}$ seconds, all the sleeping nodes switch to the listening mode, set their timers to (10), and participate

[1] A counter-based single-relay selection scheme has been proposed before in [22].

again in a new round of competition to acquire the relaying status.

Adopting the above simple policy, the K closest nodes to s act as relays while all other nodes switch to the sleeping mode to preserve energy. Moreover, the list of the K closest nodes is revised every $T^{(g)}$ seconds to adapt to possible changes in the network topology. We should stress the fact that the k-th closest node to s is not necessarily the one with the k-th largest SNR. This may result in some SNR performance degradation at the destination. However, simulation results in Section V demonstrate that this performance loss is in fact negligible in our multi-relay cooperative communication scenario.

Although the above geometry-based relay selection approach is substantially more energy efficient than its optimal SNR-based counterpart, it may over-exploit certain nodes around the source. In fact, if the network topology changes too slowly, the set of K closest nodes to the source rarely updates. Therefore, these nodes continue to switch between the listening and the transmission modes leading to an early depletion of their batteries while all the other nodes keep staying in the sleeping mode and save energy. The following relay selection scheme is proposed to reduce this detrimental effect.

3) Random Relay Selection: An approach to reduce the disparity in the nodes' remaining battery power is to periodically renew a randomly-selected group of relays from a neighborhood of radius R around s. This may be done by letting every node on $O(s,R)$, the disc of radius R centered at s, set its initial counter to a randomly generated value $T_k^{(r)} = \lambda_k^{(r)}$. When CTS is received, all the nodes on $O(s,R)$ start their countdown and the same relaying procedure as in the two previous schemes follows until the K-th relay forwards its signal. At the end of the relaying phase, all the nodes that have not succeeded to forward their signals switch to the sleeping mode for a predetermined period of $T^{(r)}$ seconds. After $T^{(r)}$ seconds elapse, all the sleeping nodes switch back to the listening mode and, together with the recent relaying set, initialize their counter values with *newly generated* random quantities. Adopting the above scheme, while a significant amount of energy is saved, all nodes on $O(s,R)$ are equally likely to acquire the relaying status over a long period of time. Hence, the risk of over-exploiting certain nodes greatly diminishes. The expense that may be incurred is the possibility of a noticeable SNR drop at the destination due to the fact that the relaying nodes are selected randomly. Note that R is a design parameter that may have a considerable effect on the performance of the random relay selection scheme. A systematic approach to choose a proper R is presented in Section IV-A3.

In the next section, we analyze the SNR performances of all proposed relay selection schemes and, in particular, derive a sufficient condition under which the energy-efficient geometry-based and random relay selection schemes result in close-to-optimal SNR performances at the destination.

IV. Performance Analysis

Hereafter, the superscripts $^{(o)}$, $^{(g)}$, and $^{(r)}$ are used to denote the SNR values corresponding to the optimal, geometry-based, and the random relay selection schemes, respectively.

A. Performance Analysis at the Relays

The SNR at the kth selected relay depends not only on the channel $h_{s,k}$, but also on the relay's distance from the source, and, therefore, both on the network topology and the approach used to select the relay. In this subsection, the relays' SNR performances of the proposed schemes are analyzed.

1) Optimal Relay Selection: The following theorem is instrumental in analyzing the performance of the optimal relay selection scheme.

Theorem 1. *Consider a WSN whose nodes are uniformly distributed according to a two-dimensional homogeneous Poisson process with intensity ρ.*[2] *Assume that the channels between the source and relays are Rayleigh fading with variance $1/2$ per dimension. Then, the CDF of the k-th largest SNR at the relays is*

$$F_{\gamma_k^{(o)}}(\gamma) = G(u(\gamma),k) \triangleq e^{-u(\gamma)} \sum_{j=0}^{k-1} \frac{u(\gamma)^j}{j!}, \qquad (11)$$

where

$$u(\gamma) = \frac{2\rho\pi}{\nu} \int_1^\infty z^{\frac{2}{\nu}-1} e^{-\frac{\gamma z}{\varsigma}} dz. \qquad (12)$$

Proof: See Appendix A. ∎

The integral in (12) is bounded and has a closed-form solution for all values of $\nu \geq 2$. In particular, $u(\gamma) = (\varsigma\rho\pi/\gamma) \cdot e^{-\gamma/\varsigma}$ for $\nu = 2$ and $u(\gamma) = (\rho\pi/2).\sqrt{\varsigma\pi/\gamma}\left(1 - \text{erf}\left(\sqrt{\gamma/(\varsigma\pi)}\right)\right)$ for $\nu = 4$ where $\text{erf}(z) \triangleq \frac{2}{\sqrt{\pi}} \int_0^z e^{-t^2} dt$. Note also that an accurate approximation of $u(\gamma)$ may be obtained by substituting the upper-bound of the integral with a large-enough but limited value and then using a variety of efficient numerical techniques to compute the result. Alternatively, given γ/ς and ρ, the kth node can obtain $u(\gamma)$ from a look-up table. Using Theorem 1, the PDF of the SNR can be found as $f_{\gamma_k^{(o)}}(\gamma) = \partial F_{\gamma_k^{(o)}}(\gamma)/\partial\gamma$, which can be used to obtain the average SNR, $\bar{\gamma}_k^{(o)}$. Note that $\bar{\gamma}_k^{(o)}$, and, hence, the normalization factor $\beta_k^{(o)}$ depend on k. Therefore, when the optimal relay selection scheme is used, each relay should know its index in the relaying queue. This knowledge can be acquired by counting the number of overheard signals transmitted from the preceding relays. Then, $\beta_k^{(o)}$ can be determined from (4).

2) Geometry-based Relay Selection: In this scheme, the nearest K nodes to the source act as relays and, hence, $h_{s,k}$ is independent from $D_{s,k}$. Therefore,

$$\bar{\gamma}_k^{(g)} = \varsigma \text{E}\left\{|h_{s,k}|^2\right\} \text{E}\left\{D_{s,k}^{-\nu}\right\} = \varsigma \text{E}\left\{D_{s,k}^{-\nu}\right\}. \qquad (13)$$

In the view of the fact that the nodes are uniformly distributed outside the unit-radius node-free zone around the source, a technique similar to that in [18] may be used to show that the PDF of $D_{s,k}$ is given by

$$f_{D_{s,k}}^{(g)}(r) = \frac{2(\rho\pi)^k}{(k-1)!} r(r^2-1)^{k-1} e^{-\rho\pi(r^2-1)} \qquad r > 1. \quad (14)$$

[2]Except a relay-free zone of unit radius around the source.

It follows from (13) and (14) that

$$\bar{\gamma}_k^{(g)} = \frac{2\varsigma(\rho\pi)^k}{(k-1)!}\int_1^\infty r^{1-\nu}(r^2-1)^{k-1}e^{-\rho\pi(r^2-1)}dr. \quad (15)$$

After some manipulations, we obtain

$$\begin{aligned}\bar{\gamma}_k^{(g)} &= \frac{\varsigma(\rho\pi)^k}{(k-1)!}\sum_{i=0}^{\infty}\binom{-\frac{\nu}{2}}{i}\int_0^\infty u^{i+k-1}e^{-\rho\pi u}du \\ &= \frac{\varsigma(\rho\pi)^k}{(k-1)!}\sum_{i=0}^{\infty}\binom{-\frac{\nu}{2}}{i}\frac{(i+k-1)!}{(\rho\pi)^{i+k}}, \end{aligned} \quad (16)$$

where $\binom{\alpha}{k} \triangleq \alpha(\alpha-1)\cdots(\alpha-k+1)/k!$. This, along with (4), indicates that the normalization factor $\beta_k^{(g)}$ also depends on k.

3) Random Relay Selection: When the relays are selected using the random selection technique, the PDF of $D_{s,k}$ is $f_{D_{s,k}}^{(r)}(r) = 2r/(R^2-1)$. Exploiting the independence between $D_{s,k}$ and $h_{s,k}$ in this relay selection scheme, it follows from (13) that

$$\bar{\gamma}_k^{(r)} = \varsigma\int_1^R \frac{2t^{1-\nu}}{R^2-1}dt = \begin{cases} \varsigma\cdot\frac{2\ln(R)}{R^2-1} & \nu = 2 \\ \varsigma\cdot\frac{2(R^{2-\nu}-1)}{(R^2-1)(2-\nu)} & \nu \neq 2 \end{cases}. \quad (17)$$

Note from (17) that $\bar{\gamma}_k^{(r)}$, and, hence, $\beta_k^{(r)}$ are independent from k. Therefore, when the random relay selection scheme is used, it is not required that the relays are aware of their position in the relaying queue.

As (17) suggests, the choice of R can have a significant impact on the performance of the random relay selection scheme. While R should not be selected very small so that there are not enough nodes on $O(s,R)$, it also should not be chosen very large so that the nodes that act as relays suffer from a long distance from s and a weak SNR problem. In what follows, the above guideline is used to propose a systematic approach to select R. First, note that $O(s,R)$ should be large enough to include at least qK nodes where the design parameter $q > 1$ guarantees that the list of K randomly-selected relays from $O(s,R)$ can be renewed to prolong the network lifetime. Second, the SNR at every selected relay on $O(s,R)$ should exceed the threshold $\gamma^\star$ to meet the required reception quality. As the relays' list is random and is also randomly renewed, the latter SNR requirement is guaranteed only if the SNRs at all nodes on $O(s,R)$ are larger than or equal to $\gamma^\star$. Now, consider the events $\mathcal{A}_l = \{\text{There are exactly } l \text{ nodes on } O(s,R)\}$ and $\mathcal{B}_l = \{\text{SNRs of all the } l \text{ nodes on } O(s,R) \text{ are larger than or equal to } \gamma^\star\}$. The radius R may be selected such that $\sum_{l=qK}^{\infty}\Pr(\mathcal{A}_l\cap\mathcal{B}_l)$, the total probability of good events, is maximized, or, equivalently, the outage probability

$$\begin{aligned}\mathrm{P}_{\text{out}}(R) &= 1 - \sum_{l=qK}^{\infty}\Pr(\mathcal{A}_l\cap\mathcal{B}_l) \\ &= 1 - \sum_{l=qK}^{\infty}\Pr(\mathcal{A}_l)\Pr(\mathcal{B}_l|\mathcal{A}_l), \end{aligned} \quad (18)$$

is minimized. As the nodes are uniformly distributed with density ρ, the number of nodes on $O(s,R)$ and outside the unit-distance node-free zone around s follows a Poisson distribution with parameter $\rho\pi(R^2-1)$. As such, $\Pr(\mathcal{A}_l) = e^{-\rho\pi(R^2-1)}\cdot(\rho\pi(R^2-1))^l/l!$. Further, as the nodes' SNRs are independent random variables, it is straightforward to show that $\Pr(\mathcal{B}_l|\mathcal{A}_l) = (1-F_{\gamma_k}(r|R))^l$ where $F_{\gamma_k}(r|R)$ is the CDF of the SNR of an arbitrary node on $O(s,R)$ and outside the unit-distance node-free zone around s and is given by (35) in Appendix A. Substituting the so-obtained $\Pr(\mathcal{A}_l)$ and $\Pr(\mathcal{B}_l|\mathcal{A}_l)$ into (18), we have

$$\mathrm{P}_{\text{out}}(R) = 1 - e^{-\rho\pi(R^2-1)}\cdot\sum_{l=qK}^{\infty}\frac{(\rho\pi(R^2-1))^l}{l!}\cdot\left(\frac{2\int_1^{R^\nu}t^{\frac{2}{\nu}-1}e^{-\frac{\gamma^\star t}{\varsigma}}dt}{\nu(R^2-1)}\right)^l. \quad (19)$$

The optimal R can then be selected as $R^\star = \underset{R}{\text{argmin}}\mathrm{P}_{\text{out}}(R)$. Fig. 2 shows $\mathrm{P}_{\text{out}}(R)$ versus R for several K and $q = 5$, $\nu = 2$, $\rho = 0.1$, $\gamma^\star = -10$ and -20 (dB), and $\varsigma = 25$ (dB). As can be observed from Fig. 2, each outage probability curve has a minimum point that corresponds to $R^\star$. Fig. 3 shows the minimum outage probability $\mathrm{P}_{\text{out}}(R^\star)$ versus the source transmission power to noise ratio ς (in dB), for $q = 5$, $\nu = 2$, $\rho = 0.1$, and several pairs of $(\gamma^\star, K)$. As expected, $\mathrm{P}_{\text{out}}(R^\star)$ is a decreasing function of ς in all cases.

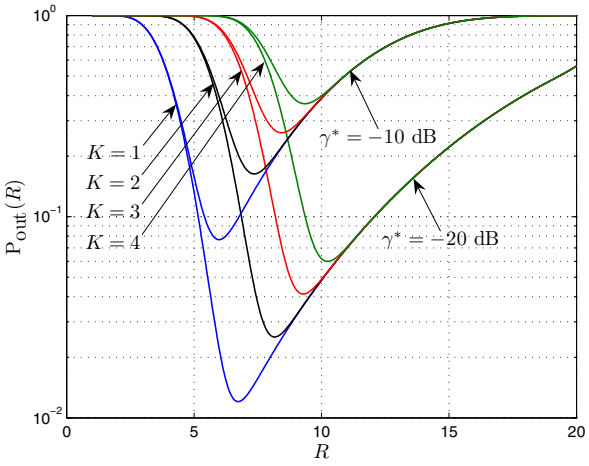

Fig. 2. $P_{out}(R)$ versus R for several K in the random relay selection scheme.

B. Performance Analysis at the Destination

It follows from (7) and (8) that the average SNR at the destination in all relay selection schemes is

$$\bar{\gamma}_d^{(\bullet)} = \sum_{k=1}^{K}\underbrace{\mathrm{E}\left\{\frac{\alpha_k^{(\bullet)}|h_{k,d}|^2}{1+\alpha_k^{(\bullet)}|h_{k,d}|^2}\right\}}_{\phi_k^{(\bullet)}}\bar{\gamma}_k^{(\bullet)} \quad (20)$$

where $\bullet$ is either "o", "g" or "r" depending on the employed relay selection scheme. As the channel coefficients $h_{k,d}, k = 1,\ldots,K$ are zero-mean Gaussian r.v.s with a variance of $1/2$ per dimension, $|h_{k,d}|^2$ are unit-mean exponentially distributed r.v.s. Therefore, $\phi_k^{(\bullet)} = \int_0^\infty \alpha_k^{(\bullet)}xe^{-x}/\left(1+\alpha_k^{(\bullet)}x\right)dx = 1-$

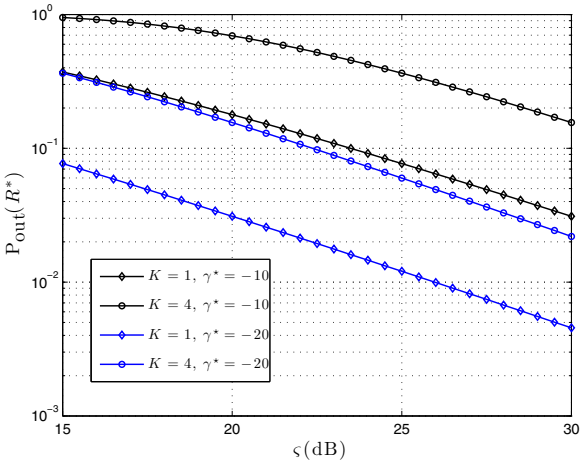

Fig. 3. $P_{out}(R^\star)$ versus ς for several pairs of $(\gamma^\star, K)$ in the random relay selection scheme.

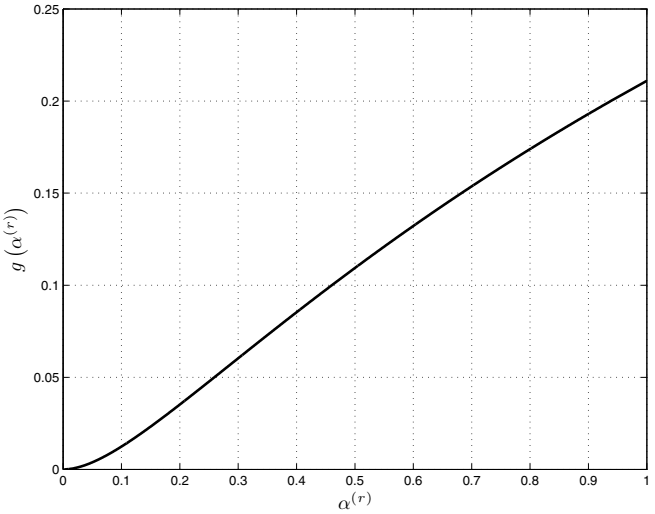

Fig. 4. $g\left(\alpha^{(r)}\right)$ versus $\alpha^{(r)}$.

$\left(\left(e^{1/\alpha_k^{(\bullet)}}\right)/\alpha_k^{(\bullet)}\right)\mathrm{E}_1\left(1/\alpha_k^{(\bullet)}\right)$ where $\mathrm{E}_1(z) \triangleq \int_z^\infty e^{-t}/t\ dt$ is the exponential integral. Using the latter result in (20) yields

$$\bar{\gamma}_d^{(\bullet)} = \sum_{k=1}^{K} \bar{\gamma}_k^{(\bullet)} \left(1 - \frac{e^{\frac{1}{\alpha_k^{(\bullet)}}}}{\alpha_k^{(\bullet)}} \mathrm{E}_1\left(\frac{1}{\alpha_k^{(\bullet)}}\right)\right). \tag{21}$$

The following remarks are in order:

1) In many practical scenarios, we have

$$\alpha_k^{(\bullet)} = \beta_k^{(\bullet)} D^{-\nu} = \frac{1}{K} \cdot \frac{P_T}{\sigma^2 D^\nu} \cdot \frac{1}{\bar{\gamma}_k^{(\bullet)} + 1} \ll 1. \tag{22}$$

Inequality (22) holds, for instance, with a moderate level of P_T/KD^ν and a high average SNR at the k-th relay. When (22) is valid, one may use the approximation $\mathrm{E}_1(z) \approx (e^{-z}/z) \cdot (1 - 1/z)$ for $z \gg 1$ in (21) and obtain

$$\bar{\gamma}_d^{(\bullet)} \approx \sum_{k=1}^{K} \bar{\gamma}_k^{(\bullet)} \alpha_k^{(\bullet)} = \frac{1}{K} \sum_{k=1}^{K} \frac{P_T}{\sigma^2 D^\nu} \cdot \frac{\bar{\gamma}_k^{(\bullet)}}{\bar{\gamma}_k^{(\bullet)} + 1}. \tag{23}$$

An important consequence of (23) is that when the average SNRs at all selected relays are high enough, that is, $\bar{\gamma}_k^{(\bullet)} \gg 1$ for $k = 1, \ldots, K$, then the average SNR at the destination can be further simplified to

$$\bar{\gamma}_d^{(\bullet)} \approx \eta_d \triangleq \frac{P_T}{\sigma^2 D^\nu}. \tag{24}$$

Interestingly, (24) is the average SNR that would be achieved at the destination if the whole WSN were replaced by a single node with a transmission power of P_T. In fact, the average SNR expression in (24) depends only on the total transmission power from the network in the relaying phase, the distance of the destination from the network, and the noise power at the destination. It is, however, independent of the relay selection scheme or the total number of relays. The above discussion reveals the simple and very useful fact that, as long as the average SNRs at all selected relays are high enough, the SNR performance at the destination is insensitive to the approach used to select the relays and, in particular, the optimal, the geometry-based, and the random relay selection schemes achieve approximately the same average SNR of η_d at the destination. In such a case, the random relay selection scheme that is both energy efficient and fair towards all nodes may be employed without compromising the performance.

2) Following our discussion, $\bar{\gamma}_k^{(r)}$, $\beta_k^{(r)}$, and, hence, $\alpha_k^{(r)}$, are independent from k. Therefore, if the random relay selection scheme is used, then, according to (21), $\bar{\gamma}_d^{(r)} = K\bar{\gamma}^{(r)}\left(1 - e^{1/\alpha^{(r)}}\mathrm{E}_1\left(1/\alpha^{(r)}\right)/\alpha^{(r)}\right)$ where k in $\gamma_k^{(r)}$ and $\alpha_k^{(r)}$ is removed to underline the independency of the latter two quantities from the relay index. Taking the partial derivative of $\bar{\gamma}_d^{(r)}$ with respect to the total number of relays K and taking into account the fact that $\gamma^{(r)}$ is independent from K, while, according to (6), $\alpha^{(r)}$ is inversely proportional to K, it can be readily shown that $\partial\bar{\gamma}_d^{(r)}/\partial K = \bar{\gamma}^{(r)} g\left(\alpha^{(r)}\right)$ where

$$g\left(\alpha^{(r)}\right) = 1 + \frac{1}{\alpha^{(r)}} - \frac{1}{\alpha^{(r)}}\left(2 + \frac{1}{\alpha^{(r)}}\right) e^{\frac{1}{\alpha^{(r)}}} \mathrm{E}_1\left(\frac{1}{\alpha^{(r)}}\right). \tag{25}$$

Fig. 4 shows $g\left(\alpha^{(r)}\right)$ as a function of $\alpha^{(r)}$. As can be observed from Fig. 4, $g\left(\alpha^{(r)}\right)$ is nonnegative and monotonically increasing with respect to $\alpha^{(r)}$. From the latter observation along with the fact that $\bar{\gamma}^{(r)}$ is a constant positive scalar, it follows that

- $\bar{\gamma}_d^{(r)}$ is an increasing function of K regardless of $\alpha^{(r)}$. As such, when the random relay selection scheme is used, increasing the number of relays K elevates the expected SNR level at the destination. This result is far from being trivial as the relays are only randomly selected and, more importantly, the average of the relays' total transmission power P_T does not change with K. Note that as P_T is fixed, a reasonable strategy to improve the average SNR at the destination in the random relay selection scheme is to lower the average transmission power from every relay in favor of increasing the total number of relays. Such a strategy additionally contributes to prolonging the nodes' lifetime.
- The larger the $\alpha^{(r)}$, the larger the increase in $\bar{\gamma}_d^{(r)}$ due to the use of one additional relay. This fact along with (6) imply that when the allocated average transmission

power to each relay P_T/K is large or the average SNR at the relays is low, adding one relay to the system has a more prominent effect on increasing $\bar{\gamma}_d^{(r)}$.

C. SNR Variance at the Destination for a Large K

It is of practical value to study the variations of $\gamma_d^{(\bullet)}$ around $\bar{\gamma}_d^{(\bullet)}$ as K increases. Using (7) and (8) along with the facts that $\alpha_k^{(\bullet)}$ is inversely proportional to K, and $h_{s,k}$ and $h_{k,d}$ are independent r.v.s, it can be readily shown that

$$\mathrm{var}\left(\gamma_d^{(\bullet)}\right) = \frac{\zeta_1^{(\bullet)}}{K} + \zeta_2^{(\bullet)} F_K^{(\bullet)} \tag{26}$$

where $\zeta_1^{(\bullet)}$ and $\zeta_2^{(\bullet)}$ are two scalars independent from K and

$$F_K^{(\bullet)} = \frac{1}{\varsigma^2 K^2} \sum_{m=1}^{K} \sum_{l=1}^{m-1} \mathrm{E}\left\{\gamma_l^{(\bullet)} \gamma_m^{(\bullet)}\right\} - \mathrm{E}\left\{\gamma_l^{(\bullet)}\right\} \mathrm{E}\left\{\gamma_m^{(\bullet)}\right\}. \tag{27}$$

As can be observed from (27), in general, $F_K^{(\bullet)}$ depends on the joint PDF of the SNRs of the selected relays. In the following, $F_K^{(\bullet)}$ in the optimal, the geometry-based, and the random relay selection schemes is analyzed and the behavior of $\mathrm{var}\left(\gamma_d^{(\bullet)}\right)$ when K grows large is investigated.

1) Optimal Relay Selection: As mentioned before, studying $\mathrm{var}\left(\gamma_d^{(o)}\right)$ requires the knowledge of $f_{\gamma_m^{(o)},\gamma_l^{(o)}}(.,.)$, the joint PDF of $\gamma_l^{(o)}$ and $\gamma_m^{(o)}$. The following theorem derives the latter function.

Theorem 2. *For $m > l$, the joint PDF of $\gamma_l^{(o)}$ and $\gamma_m^{(o)}$ is given by* (28) *at the top of the next page, where $G(\cdot,\cdot)$ is defined in* (11)*.*

Proof: See Appendix B. ∎

Using (11) and (28), analytical expressions of $\mathrm{E}\left\{\gamma_l^{(o)}\right\}$ and $\mathrm{E}\left\{\gamma_l^{(o)}\gamma_m^{(o)}\right\}$ can be obtained and then used to derive $F_K^{(o)}$. Although $F_K^{(o)}$ is a rather complicated function (not given here), the simulation results shown in Fig. 5 verify that $\left|F_K^{(o)}\right|$ is a decreasing function of K for the tested values of ν and ρ. The latter observation along with (27) suggest that $\mathrm{var}\left(\gamma_d^{(o)}\right)$ should converge to zero as the number of relays increases.

2) Geometry-based Relay Selection: In the geometry-based relay selection scheme where $h_{s,k}$ and $D_{s,k}$ are independent for every k, $F_K^{(g)}$ may be written as

$$F_K^{(g)} = \frac{1}{K^2} \sum_{m=1}^{K} \sum_{l=1}^{m-1} \mathrm{E}\left\{D_{s,l}^{-\nu} D_{s,m}^{-\nu}\right\} - \mathrm{E}\left\{D_{s,l}^{-\nu}\right\} \mathrm{E}\left\{D_{s,m}^{-\nu}\right\}. \tag{29}$$

The analysis of $\mathrm{var}\left(\gamma_d^{(g)}\right)$ requires the knowledge of $f^{(g)}_{D_{s,l},D_{s,m}}(\cdot,\cdot)$, the joint PDF of the source-node distances of the lth and mth closest nodes to the source. The following theorem holds.

Theorem 3. *For $m > l$, the joint PDF of $D_{s,l}$ and $D_{s,m}$ in the geometry-based relay selection scheme is given by* (30) *at the top of the next page.*

Proof: See Appendix C . ∎

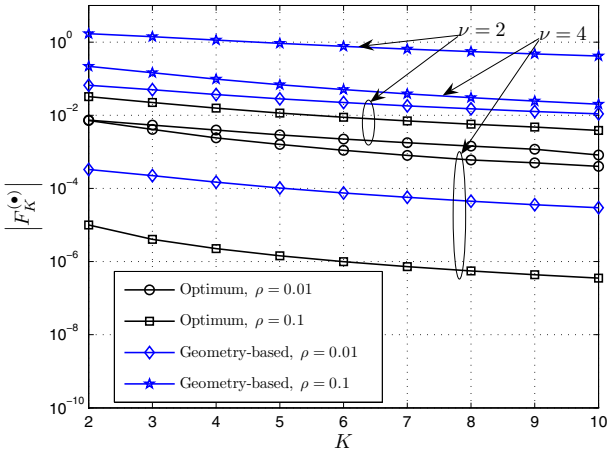

Fig. 5. $\left|F_K^{(o)}\right|$ and $\left|F_K^{(g)}\right|$ versus K for $\varsigma = 25$ (dB), $\rho = 0.1$ and $\rho = 0.01$.

The joint PDF in (30) facilitates computing $F_K^{(g)}$ from (29). The simulation results shown in Fig. 5 verify the decreasing behavior of $\left|F_K^{(g)}\right|$ as K grows. This observation suggests that $\mathrm{var}\left(\gamma_d^{(g)}\right)$ should also converge to zero as K increases.

3) Random Relay Selection: In the random relay selection scheme, not only are $h_{s,k}$ and $D_{s,k}$ independent for every k, but also $D_{s,k}$, $k = 1,\ldots,K$ are independent across k. Therefore, $\mathrm{E}\left\{\gamma_l^{(r)}\gamma_m^{(r)}\right\} = \mathrm{E}\left\{\gamma_l^{(r)}\right\}\mathrm{E}\left\{\gamma_m^{(r)}\right\}$ and, hence, $F_K^{(r)} = 0$. Then, it directly follows from (26) that $\mathrm{var}\left(\gamma_d^{(r)}\right)$ converges to zero with rate $\mathcal{O}(1/K)$.

Convergence of $\mathrm{var}\left(\gamma_d^{(\bullet)}\right)$ to zero implies that if K is large enough, then, for any arbitrary set of realizations of $D_{s,k}$, $h_{s,k}$, and $h_{k,d}$, $\gamma_d^{(\bullet)}$ should be close to $\bar{\gamma}_d^{(\bullet)}$. This confirms that $\bar{\gamma}_d^{(\bullet)}$ is a sensible performance measure for the considered cooperative WSN and the derived properties of the average SNR at the destination also approximately hold for the instantaneous SNR at this terminal. Moreover, the above result verifies that the proposed relay selection schemes effectively decrease the signal power fluctuations at the destination. This is an expected effect due to the spatial diversity provided by the K independent channel paths.

V. Simulations

In this section, further numerical simulations are used to validate the analytical results. Fig. 6 shows the analytical and numerical $\bar{\gamma}_d^{(r)}$, $\bar{\gamma}_d^{(g)}$, and $\bar{\gamma}_d^{(o)}$ versus K for $D = 1000$, $R = 20$, $\nu = 2$, $\sigma^2 = 1$, $\rho = 1$, $\eta_d = P_T/(\sigma^2 D^\nu) = 15$ (dB), and two different $\eta_s \triangleq p_s/(\sigma^2 R^\nu) = 0$ (dB) and 7 (dB). Note that η_s is the average SNR on the boundary of $O(s,R)$, and, therefore, $\bar{\gamma}_k^{(r)} \geq \eta_s$ for $k = 1,2,...,K$. The figure shows the results of averaging over 10^5 random realizations of the channel links and source-relay distances. Fig. 6 further verifies that the derived average SNR expressions accurately predict their numerical counterparts.

Fig. 7 shows the analytical and numerical $\bar{\gamma}_d^{(r)}$, $\bar{\gamma}_d^{(g)}$, and $\bar{\gamma}_d^{(o)}$ versus η_s for $\rho = 1$ and $K = 10$. In Fig. 7, $\eta_d = 15$ (dB) is also plotted as a reference. As can be observed from

$$f_{\gamma_m^{(o)},\gamma_l^{(o)}}(x,y) = \begin{cases} \dfrac{\partial}{\partial x} G\left(u(x)-u(y), m-l\right) \cdot \dfrac{\partial}{\partial y} G\left(u(y), l\right) & y \geq x \\ 0 & y < x \end{cases} \tag{28}$$

$$f^{(g)}_{D_{s,l},D_{s,m}}(r,t) = \begin{cases} 4(\rho\pi)^m \cdot \dfrac{t(t^2-1)^{m-l-1}}{(m-l-1)!} \cdot \dfrac{r(r^2-1)^{l-1}}{(l-1)!} \cdot \left(\dfrac{t^2-r^2}{t^2-1}\right)^{m-l-1} \cdot e^{-\rho\pi(t^2-1)} & t \geq r \\ 0 & t < r \end{cases} \tag{30}$$

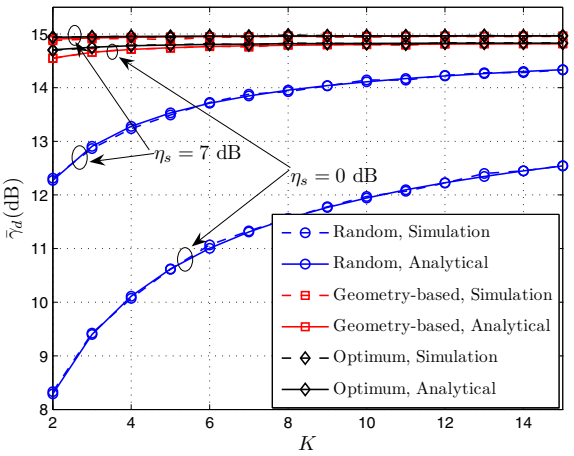

Fig. 6. $\bar{\gamma}_d$ versus K for $\rho = 1$, $\eta_d = 15$ (dB), and $\eta_s = 0$ and $\eta_s = 7$ (dB).

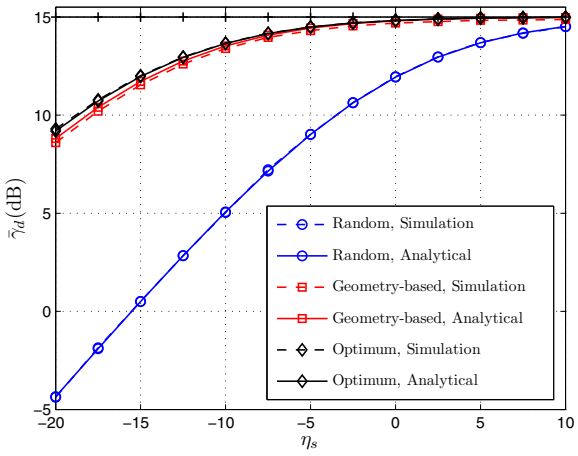

Fig. 7. $\bar{\gamma}_d$ versus η_s for $\rho = 1$, $K = 10$, and $\eta_d = 15$ (dB).

the figure, the numerical results very closely follow their analytical counterparts and when η_s is very small, $\bar{\gamma}_d^{(o)}$ and $\bar{\gamma}_d^{(g)}$ are noticeably higher than $\bar{\gamma}_d^{(r)}$. However, increasing η_s, all $\bar{\gamma}_d^{(r)}$, $\bar{\gamma}_d^{(g)}$, and $\bar{\gamma}_d^{(o)}$ rapidly increase and converge to η_d. Corroborating the result in IV-B, this demonstrates that if the average SNRs at all relays are large enough, the average SNR at the destination approaches η_d regardless of the selected relaying set. This figure also shows that $\bar{\gamma}_d^{(g)}$ is very close to $\bar{\gamma}_d^{(o)}$ for an extended range of η_s starting as low as -20 (dB). The latter observation verifies the close-to-optimal performance of the geometry-based relay selection scheme even at a very low SNR regime. Note also that $\bar{\gamma}_d^{(r)}$ enters the one-dB vicinity of η_d at moderate $\eta_s \approx 5$ (dB).

The analytical and numerical $\bar{\gamma}_d^{(r)}$ and $\bar{\gamma}_d^{(g)}$ are shown versus ρ in Fig. 8 for $K = 10$ and $\eta_s = 5$ (dB) and $\eta_s = 10$ (dB). As can be observed from the figure, $\bar{\gamma}_d^{(r)}$ is insensitive to ρ. This is an expected fact due to the independency of $\bar{\gamma}_k^{(r)}$ in (17) from ρ. Note that $\bar{\gamma}_d^{(g)}$ and $\bar{\gamma}_d^{(o)}$ are increasing functions of ρ. This property can be readily justified as the larger the ρ, the higher the probability of finding K nodes at a closer distance to the source.

The receiver bit error rate (BER) curves versus η_s are plotted in Fig. 9 for the 4-quadrature amplitude modulation (QAM) and $\rho = 1$, $\eta_d = 15$ (dB), and both $K = 5$ and $K = 10$. The BER curves in Fig. 9 demonstrate the receiver performance improvements as one migrates from the random to the geometry-based and then to the optimal relay selection scheme. The floor levels of the BER curves are due to the fact

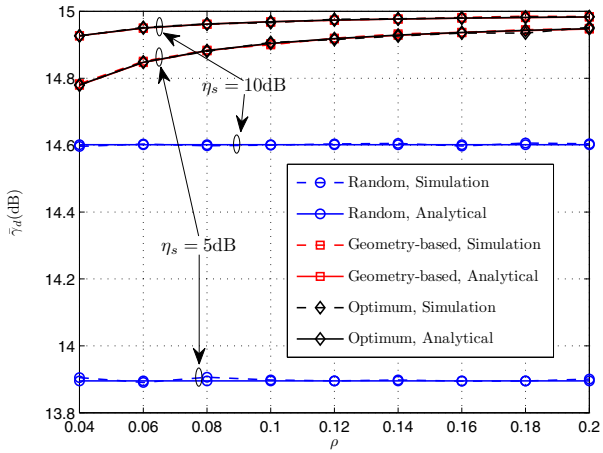

Fig. 8. $\bar{\gamma}_d$ versus ρ for $K = 10$, $\eta_d = 15$ (dB) and $\eta_s = 5$ (dB) and $\eta_s = 10$ (dB).

that η_d is fixed, and, hence, the relays forward channels do not strengthen as η_s increases.

The next experiment investigates the energy efficiency of the proposed relay selection schemes. We consider a WSN with $N = 440$ nodes that are uniformly distributed in a square with the side of 20 meters at time $t = 0$. The transmitter is located at the center of the square at $(0, 0)$. To model the nodes movements, each node's position changes after every transmission time according to a random walk with step size $d_s = 0.05$ in both x and y directions, that is, the node n located at $(x_t, y_t)_n$ at time t moves to one of the four

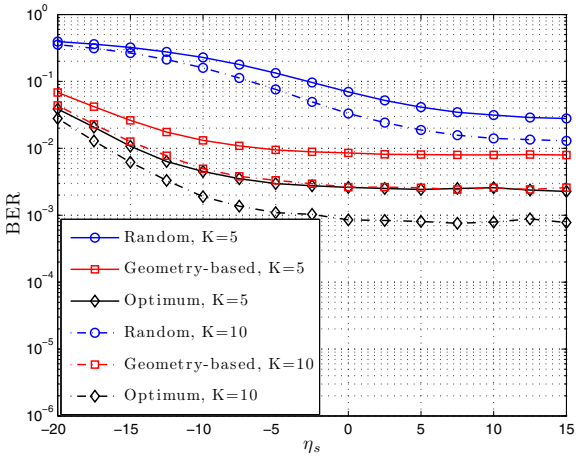

Fig. 9. BER versus η_s for $\rho = 1$ and $\eta_d = 15$ (dB).

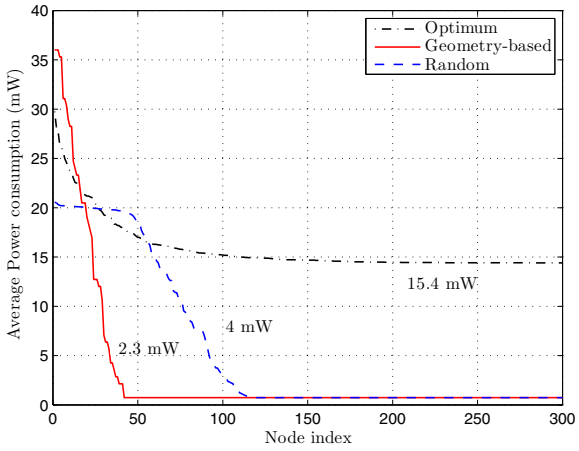

Fig. 10. The nodes average power consumptions in the decreasing order after 1000 transmission times. The number close to each curve shows the total average power consumption of the network in the corresponding scheme.

points $(x_t \pm d_s, y_t \pm d_s)_n$ with equal probabilities. The power consumption of each node in the transmission, listening, and sleeping mode are assumed to be $P_t = 36$ mW, $P_l = 14.4$ mW and $P_s = 15$ μW, respectively [26]. We assume that both $T^{(g)}$ and $T^{(r)}$ are equal to 20 transmission times and select $K = 20$ relaying nodes according to the optimal, geometry-based, and random relay selection schemes. Fig. 10 shows the nodes average power consumptions in the decreasing order after 1000 transmission times (for a better illustration, only the first 300 nodes with the highest average power consumptions are shown). The horizontal axis in Fig. 10 indicates the power consumption rank of the node, that is, one indicates the node with the highest power consumption, two indicates the node with the second highest power consumption and so on. The number close to each curve shows the total average power consumption of the network in the corresponding scheme. As can be observed from Fig. 10, the total average power consumption in the optimal relay selection scheme is substantially higher than those in the geometry-based and the random selection schemes. As discussed in Section III, this is due to the fact that nodes do not go to the sleeping mode in the optimal scheme. The geometry-based scheme significantly reduces the network average power consumption by keeping most nodes in the sleeping mode. However, as Fig. 10 shows, only a small percentage of the nodes spend most of the total power. This verifies our discussion in Section III that, although energy-efficient, the geometry-based scheme tend to over-exploit the nodes that remain mainly around the source. Fig. 10 shows that the latter problem is solved in the random relay selection scheme where the nodes' maximal average power consumption is much lower than that in the geometry-based scheme and more nodes act as relays sometime during the examined 1000 transmission times. It can also be observed that the total average power consumption in the random relay selection scheme is slightly higher than that in its geometry-based counterpart. This is due to the fact that, in the random relay selection scheme, more nodes remain in the listening mode at every transmission time to compete for acquiring the relaying status. Note that the tail of the plot of the geometry-based (the random) relay selection technique remains constant at a very low level that is equal to the listening power consumption of the nodes at every $T^{(g)}$ (or $T^{(r)}$) transmission time.

VI. Conclusions

Three decentralized relay selection techniques have been proposed for wireless sensor networks with uniformly distributed nodes in the case that the forward channels' information is not available at the nodes: 1) The optimal relay selection scheme where K nodes with the highest instantaneous SNRs act as relays. This technique is SNR-optimal among all relay selection techniques that do not use any information regarding the nodes' forward channels but is energy-inefficient due to its requirement to keep the nodes in the active listening or transmission modes. 2) The geometry-based relay selection scheme that ignores the instantaneous channel variations and chooses K closest nodes to the source as relays. While achieving a close-to-optimal average SNR at the destination, this scheme is energy-efficient as the non-relaying nodes may be left in the sleeping mode most of the time. The main disadvantage of the geometry-based relay selection technique is its tendency to over-exploit the group of nodes that stay close to the source in networks with a more static topology. 3) The energy-efficient and fair but, possibly, noticeably suboptimal random relay selection technique that randomly selects the K relays from the nodes in an R-neighborhood of the source. Defining a suitable outage probability, a systematic approach to select R has also been proposed. It has been shown that randomly selecting additional relays can increase the average SNR at the destination while further improving the network lifetime due to a less transmission power from each individual relay.

The average SNR performances of the proposed techniques have been analyzed both at the relays and the destination and a sufficient condition has been obtained under which the average SNR at the destination becomes independent from the used relay selection technique. The SNR variance at the destination has also been analytically studied. Various

numerical simulations have been used to verify the analytical results.

APPENDIX A

The proof of Theorem 1 is accomplished in four steps as follows.

Step 1: Consider an arbitrary node k that is located on the ring centered at s and with the outer radius A and the inner radius[3] 1. Equation (2) may be rewritten as

$$\gamma_k = \frac{|H_{s,k}|^2}{D_{s,k}^{\nu}} \tag{31}$$

where $H_{s,k} \triangleq \sqrt{\varsigma} h_{s,k}$. As $h_{s,k}$ is a Rayleigh fading channel coefficient with the variance $1/2$ per dimension, $|H_{s,k}|^2$ is exponentially distributed with the parameter $1/\varsigma$, that is, $f_{|H_{s,k}|^2}(r) = \frac{1}{\varsigma} e^{-\frac{r}{\varsigma}}$. Moreover, as the nodes are uniformly distributed on the ring, it is straightforward to show that the PDF of $D_{s,k}^{-\nu}$ is $f_{D_{s,k}^{-\nu}}(r|A) = \frac{2r^{-\frac{2}{\nu}-1}}{\nu(A^2-1)}$. Using the above results, the PDF of γ_k can be computed as follows:

$$\begin{aligned} f_{\gamma_k}(r|A) &= \frac{d}{dr}\Pr\left\{|H_k|^2 D_{s,k}^{-\nu} \le r\right\} \\ &= \frac{d}{dr}\int_{A^{-\nu}}^{1} \frac{2x^{-\frac{2}{\nu}-1}}{\nu\left(A^2-1\right)} \int_0^{\frac{r}{x}} \frac{1}{\varsigma} e^{-\frac{y}{\varsigma}} dy dx \\ &= \int_{A^{-\nu}}^{1} \frac{2x^{-\frac{2}{\nu}-1}}{\nu\left(A^2-1\right)} \cdot \frac{1}{\varsigma} e^{-\frac{r}{\varsigma x}} \cdot \frac{1}{x} dx \qquad (32) \\ &= \frac{2}{\nu\varsigma\left(A^2-1\right)} \int_1^{A^{\nu}} z^{\frac{2}{\nu}} e^{-\frac{rz}{\varsigma}} dz \qquad (33) \end{aligned}$$

where the second line holds due to the fact that $D_{s,k}^{-\nu}$ and $|H_{s,k}|^2$ are independent. From (33), the CDF of γ_k is

$$\begin{aligned} F_{\gamma_k}(r|A) &= \frac{1}{\nu\varsigma\left(A^2-1\right)} \int_0^r \int_1^{A^{\nu}} z^{\frac{2}{\nu}} e^{-\frac{\xi z}{\varsigma}} d\xi dz \qquad (34) \\ &= 1 - \frac{2}{\nu\left(A^2-1\right)} \int_1^{A^{\nu}} z^{\frac{2}{\nu}-1} e^{-\frac{rz}{\varsigma}} dz. \qquad (35) \end{aligned}$$

Step 2: Let N be the total number of nodes on the ring with the center at s and the outer radius A and the inner radius 1. As $\gamma_1, \gamma_2, \ldots, \gamma_N$ are independent and identically distributed (i.i.d.), the results from the order statistics can be used to show that the PDF of the k largest r.v. in $\gamma_1, \ldots, \gamma_N$ is

$$\begin{aligned} f_{\gamma_{(k)}}(r|A) = \frac{N!}{(k-1)!(N-k)!} F_{\gamma_k}^{N-k}(r|A) \times \\ \left(1 - F_{\gamma_k}(r|A)\right)^{k-1} f_{\gamma_k}(r|A) \end{aligned} \tag{36}$$

where $f_{\gamma_k}(r|A)$ and $F_{\gamma_k}(r|A)$ are given by (33) and (35), respectively.

Step 3: As the WSN nodes are uniformly distributed over a large area, the PDF of $\gamma_k^{(o)}$ can be computed as

$$f_{\gamma_k^{(o)}}(r) = \lim_{\substack{A\to\infty \\ (N/\pi A^2)\to\rho}} f_{\gamma_{(k)}}(r|A). \tag{37}$$

From the latter equality along with (33)-(36) we have (38) at the top of the next page. Equation (38) directly yields (39), where $u(r)$ is given by (12) and $du(r)/dr = -2\rho\pi/(\nu\varsigma) \cdot \int_1^{\infty} z^{2/\nu} e^{-rz/\varsigma} dz$ is used in the second equality.

Step 4: It remains to obtain $F_{\gamma_k^{(o)}}(r) = -\int_0^r \frac{1}{(k-1)!} e^{-u(\xi)} u(\xi)^{k-1} du(\xi)$. Introducing $t \triangleq u(\xi)$, we have

$$\begin{aligned} F_{\gamma_k^{(o)}}(r) &= -\int_{u(0)}^{u(r)} \frac{1}{(k-1)!} e^{-t} t^{k-1} dt \qquad (40) \\ &= \int_{u(r)}^{\infty} \frac{1}{(k-1)!} e^{-t} t^{k-1} dt \\ &= -e^{-t} \sum_{l=0}^{k-1} \frac{t^l}{l!} \Bigg]_{u(r)}^{\infty} \qquad (41) \\ &= e^{-u(r)} \sum_{l=0}^{k-1} \frac{u(r)^l}{l!} = G(u(r), k). \qquad (42) \end{aligned}$$

This completes the proof.

APPENDIX B

When $m > l$, we have $f_{\gamma_m^{(o)}, \gamma_l^{(o)}}(x, y) = 0$ for $x > y$ and

$$f_{\gamma_m^{(o)}, \gamma_l^{(o)}}(x, y) = f_{\gamma_m^{(o)}|\gamma_l^{(o)}}(x|y) \cdot f_{\gamma_l^{(o)}}(y) \tag{43}$$

for $x \le y$. According to Theorem 1, $f_{\gamma_l^{(o)}}(y) = \partial G(u(y), l)/\partial y$. To compute $f_{\gamma_m^{(o)}|\gamma_l^{(o)}}(x|y)$, assume that N nodes are uniformly distributed on the ring with the center at s, the outer radius A, and the inner radius 1 and denote the k-th largest SNR at those nodes as $\gamma_{(k)}$. Then we have

$$\begin{aligned} f_{\gamma_m^{(o)}|\gamma_l^{(o)}}(x|y) &= \frac{\partial}{\partial x} P\left\{\gamma_m^{(o)} \le x | \gamma_l^{(o)} = y\right\} \qquad (44) \\ &= \lim_{\substack{A\to\infty \\ (N/\pi A^2)\to\rho}} \frac{\partial}{\partial x} P\left\{\gamma_{(m)} \le x | \gamma_{(l)} = y, A\right\}. \qquad (45) \end{aligned}$$

In (44), $P\left\{\gamma_{(m)} \le x|\gamma_{(l)} = y, A\right\}$ is equal to $P\left\{\gamma_{(m)} \le x\right\}$ given that the SNRs of $N-l$ nodes on the ring are not larger than y. Consider the latter $N-l$ nodes and denote their SNRs as $\gamma_1^y, \ldots, \gamma_{N-l}^y$ where the indexing is arbitrary. The m-th largest SNR $\gamma_{(m)}$ among the original set of SNRs $\gamma_1, \ldots, \gamma_N$ is the $m-l$-th largest SNR among $\gamma_1^y, \ldots, \gamma_{N-l}^y$. Therefore, $P\left\{\gamma_{(m)} \le x|\gamma_{(l)} = y, A\right\}$ is given by $P\left\{\gamma_{(m-l)}^y \le x\right\}$ where $\gamma_{(m-l)}^y$ is the $m-l$-th largest entry among $\gamma_1^y, \ldots, \gamma_{N-l}^y$. Using the latter result in (44), we have

$$\begin{aligned} f_{\gamma_m^{(o)}|\gamma_l^{(o)}}(x|y) &= \lim_{\substack{A\to\infty \\ (N/\pi A^2)\to\rho}} \frac{\partial}{\partial x} P\left\{\gamma_{(m)} \le x | \gamma_{(l)} = y, A\right\} \qquad (46) \\ &= \lim_{\substack{A\to\infty \\ (N/\pi A^2)\to\rho}} f_{\gamma_{(m-l)}^y}(x|A). \qquad (47) \end{aligned}$$

The following results are essential to derive $f_{\gamma_{(m-l)}^y}(x|A)$: 1) All $\gamma_1^y, \ldots, \gamma_{N-l}^y$ belong to $\{\gamma_1, \ldots, \gamma_N\}$ with the only distinction that they are known to be not larger than y. Therefore, similar to $\gamma_1, \ldots, \gamma_N$, the $N-l$ r.v.s $\gamma_1^y, \ldots, \gamma_{N-l}^y$

[3]The inner radius is to account for the node-free zone of unit distance around s.

$$f_{\gamma_k^{(o)}}(r) = \lim_{N\to\infty} \frac{N(N-1)\cdots(N-k+1)}{(k-1)!} \left(1 - \frac{2}{\nu\left(\frac{N}{\rho\pi}-1\right)} \int_1^{\left(\frac{N}{\rho\pi}\right)^{\frac{\nu}{2}}} z^{\frac{2}{\nu}-1} e^{-\frac{rz}{\varsigma}} dz\right)^{N-k} \cdot \left(\frac{2}{\nu\left(\frac{N}{\rho\pi}-1\right)} \int_1^{\left(\frac{N}{\rho\pi}\right)^{\frac{\nu}{2}}} z^{\frac{2}{\nu}-1} e^{-\frac{rz}{\varsigma}} dz\right)^{k-1} \cdot \left(\frac{2}{\nu\varsigma\left(\frac{N}{\rho\pi}-1\right)} \int_1^{\left(\frac{N}{\rho\pi}\right)^{\frac{\nu}{2}}} z^{\frac{2}{\nu}} e^{-\frac{rz}{\varsigma}} dz\right). \quad (38)$$

$$\begin{aligned} f_{\gamma_k^{(o)}}(r) &= \lim_{N\to\infty} \frac{1}{(k-1)!} \left(1 - \frac{\frac{2\rho\pi}{\nu}}{N} \int_1^{\infty} z^{\frac{2}{\nu}-1} e^{-\frac{rz}{\varsigma}} dz\right)^{N} \cdot \left(\frac{2\rho\pi}{\nu} \int_1^{\infty} z^{\frac{2}{\nu}-1} e^{-\frac{rz}{\varsigma}} dz\right)^{k-1} \cdot \left(\frac{2\rho\pi}{\nu\varsigma} \int_1^{\infty} z^{\frac{2}{\nu}} e^{-\frac{rz}{\varsigma}} dz\right) \\ &= -\lim_{N\to\infty} \frac{1}{(k-1)!} \left(1 - \frac{u(r)}{N}\right)^{N} u(r)^{k-1} \frac{du(r)}{dr} = -\frac{1}{(k-1)!} e^{-u(r)} u(r)^{k-1} \frac{du(r)}{dr} \end{aligned} \quad (39)$$

are also i.i.d.; 2) For any $k \in \{1, \ldots, N-L\}$ and $x \le y$, we have

$$F_{\gamma_k^y}(x|A) = P\{\gamma_k \le x | \gamma_k \le y, A\} \quad (48)$$

$$= \frac{P\{\gamma_k \le x, \gamma_k \le y | A\}}{P\{\gamma_k \le y | A\}} = \frac{F_{\gamma_k}(x|A)}{F_{\gamma_k}(y|A)} \quad (49)$$

and, hence, $f_{\gamma_k^y}(x|A) = f_{\gamma_k}(x|A)/F_{\gamma_k}(y|A)$ where $f_{\gamma_k}(x|A)$ and $F_{\gamma_k}(x|A)$ are given in (33) and (35), respectively. As $\gamma_1^y, \ldots, \gamma_{N-l}^y$ are i.i.d., the results from the order statistics can be used to show that

$$f_{\gamma_{(m-l)}^y}(x|A) = \frac{(N-l)!}{(m-l-1)!(N-m)!} \cdot F_{\gamma_k^y}^{N-m}(x|A) \times \left(1 - F_{\gamma_k^y}(x|A)\right)^{m-l-1} f_{\gamma_k^y}(x|A) \quad (50)$$

and, therefore, we have (51) in the next page. Using (33) and (35) in (51) and following a similar procedure as in (38)-(39), it can be shown that

$$f_{\gamma_m^{(o)}|\gamma_l^{(o)}}(x|y) \quad (52)$$

$$= -\frac{1}{(m-l-1)!} e^{-(u(x)-u(y))} (u(x)-u(y))^{m-l-1} \frac{du(x)}{dx}$$

$$= \frac{\partial}{\partial x} \left\{ e^{-(u(x)-u(y))} \sum_{n=0}^{m-l-1} \frac{(u(x)-u(y))^n}{n!} \right\} \quad (53)$$

$$= \frac{\partial}{\partial x} G(u(x)-u(y), m-l) \quad (54)$$

where $u(\cdot)$ and $G(\cdot,\cdot)$ are given in (12) and (11), respectively. Substituting $f_{\gamma_l^{(o)}}(y) = \partial G(u(y), l)/\partial y$ and $f_{\gamma_m^{(o)}|\gamma_l^{(o)}}(x|y)$ from (54) into the right-hand side of (43) establishes Theorem 2.

APPENDIX C

To prove (30), first note that when $m > l$, we have $f_{D_{s,l},D_{s,m}}^{(g)}(r,t) = 0$ for $t < r$ and

$$f_{D_{s,l},D_{s,m}}^{(g)}(r,t) = f_{D_{s,l}|D_{s,m}}^{(g)}(r|t) \cdot f_{D_{s,m}}^{(g)}(t) \qquad t \ge r \quad (55)$$

where $f_{D_{s,m}}^{(g)}(t)$ is given by (14). It holds that

$$f_{D_{s,l}|D_{s,m}}^{(g)}(r|t) = \frac{d}{dr} P\{D_{s,l} \le r | D_{s,m} = t\} \quad (56)$$

$$= -\frac{d}{dr} \sum_{i=0}^{l-1} P\{i \text{ nodes are inside } O(s,r) | D_{s,m} = t\}. \quad (57)$$

In (57), $P\{i \text{ nodes are inside } O(s,r)|D_{s,m}=t\}$ is the probability that i nodes are inside $O(s,r)$ given the fact that the distance of the m-th closest node to s is equal to t. This probability is equal to the probability that among the $m-1$ nodes inside $O(s,t)$, i nodes are inside $O(s,r)$ and the remaining $m-1-i$ nodes are inside or on the inner boundary of the ring centered at s with the inner radius r and the outer radius t. Therefore, given that the nodes are uniformly distributed inside $O(s,t)$, we have

$$P\{i \text{ nodes are inside } O(s,r)|D_{s,m}=t\} = \binom{m-1}{i} \left(\frac{r^2-1}{t^2-1}\right)^i \left(1 - \frac{r^2-1}{t^2-1}\right)^{m-1-i}. \quad (58)$$

Using (58) in (57) yields

$$f_{D_{s,l}|D_{s,m}}^{(g)}(r|t)$$

$$= -\frac{d}{dr} \sum_{i=0}^{l-1} \binom{m-1}{i} \left(\frac{r^2-1}{t^2-1}\right)^i \left(1 - \frac{r^2-1}{t^2-1}\right)^{m-1-i} \quad (59)$$

$$= -\frac{d}{dr} F\left(l-1; m-1, \frac{r^2-1}{t^2-1}\right) \quad (60)$$

where $F\left(l-1; m-1, (r^2-1)/(t^2-1)\right)$ is the CDF of the Binomial distribution with $l-1$ successes out of $m-1$ trials with the success probability of $(r^2-1)/(t^2-1)$. To simplify the derivative in (60), we may use the integral formula for the Binomial distribution as follows:

$$F\left(l-1; m-1, \frac{r^2-1}{t^2-1}\right) = (m-l)\binom{m-1}{l-1} \int_0^{1-\frac{r^2-1}{t^2-1}} x^{m-l-1}(1-x)^{l-1} dx. \quad (61)$$

$$f_{\gamma_m^{(o)}|\gamma_l^{(o)}}(x|y) = \lim_{\substack{A\to\infty \\ (N/\pi A^2)\to\rho}} \frac{(N-l)!F_{\gamma_k}^{N-m}(x|A)(F_{\gamma_k}(y|A)-F_{\gamma_k}(x|A))^{m-l-1}f_{\gamma_k}(x|A)}{(m-l-1)!(N-m)!(F_{\gamma_k}(y|A))^{N-l}}. \quad (51)$$

Substituting (61) in (60) and taking the derivative, we obtain

$$f_{D_{s,l}|D_{s,m}}^{(g)}(r|t) = \frac{2(m-l)r}{t^2-1}\cdot\binom{m-1}{l-1}\times \left(1-\frac{r^2-1}{t^2-1}\right)^{m-l-1}\left(\frac{r^2-1}{t^2-1}\right)^{l-1}. \quad (62)$$

Using (14) and (62) in (55) and following some straightforward manipulations, (30) is obtained.

REFERENCES

[1] Q. F. Zhou and F. C. M. Lau, "Performance bounds of opportunistic cooperative communications with CSI-assisted amplify-and-forward relaying and MRC reception," *IEEE Trans. Veh. Technol.,* vol. 59, pp. 2159–2165, June 2010.

[2] S. S. Ikki and M. H. Ahmed, "Performance analysis of adaptive decode-and-forward cooperative diversity networks with best-relay selection," *IEEE Trans. Commun.,* vol. 58, pp. 64–72, Jan. 2010.

[3] S. Lee, M. Han, and D. Hong, "Average SNR and ergodic capacity analysis for opportunistic DF relaying with outage over Rayleigh fading channels," *IEEE Trans. Wireless Commun.,* vol. 8, pp. 3890–3895, Aug. 2009.

[4] A. K. Sadek, Z. Han, and K. J. R. Liu, "Distributed relay-assignment protocols for coverage expansion in cooperative wireless networks," *IEEE Trans. Mobile Comput.,* vol. 9, pp. 505–515, Apr. 2010.

[5] A. Bletsas, H. Shin, and M. Z. Win, "Cooperative communications with outage-optimal opportunistic relaying," *IEEE Trans. Wireless Commun.,* vol. 6, pp. 3013–3025, Sep. 2007.

[6] X. Chen, T. Siu, Q. F. Zhou, and F. C. M. Lau, "High-SNR analysis of opportunistic relaying based on the maximum harmonic mean selection criterion," *IEEE Signal Process. Lett.,* vol. 17, pp. 719–722, Aug. 2010.

[7] J. N. Laneman and G. W. Wornell, "Distributed space-time coded protocols for exploiting cooperative diversity in wireless networks," *IEEE Trans. Inf. Theory,* vol. 49, pp. 2415–2425, Oct. 2003.

[8] P. A. Anghel and M. Kaveh, "Exact symbol error probability of a cooperative network in a Rayleigh-fading environment," *IEEE Trans. Wireless Commun.,* vol. 3, pp. 1416–1421, Sep. 2004.

[9] K. G. Seddik, A. K. Sadek, W. Su, and K. J. R. Liu, "Outage analysis and optimal power allocation for multinode relay networks," *IEEE Signal Process. Lett.,* vol. 14, pp. 377–380, June 2007.

[10] R. Madan, N. B. Mehta, A. F. Molisch, and J. Zhang, "Energy-efficient cooperative relaying over fading channels with simple relay selection," *IEEE Trans. Wireless Commun.,* vol. 7, pp. 3013–3025, Aug. 2008.

[11] Y. Jing and H. Jafarkhani, "Single and multiple relay selection schemes and their achievable diversity orders," *IEEE Trans. Wireless Commun.,* vol. 8, pp. 1414–1423, Mar. 2009.

[12] C. K. Lo, S. Vishwanath, and R. W. Heath, Jr., "Relay subset selection in wireless networks using partial decode-and-forward transmission," *IEEE Trans. Veh. Technol.,* vol. 58, pp. 692–704, Feb. 2009.

[13] X. Zhang, A. Ghrayeb, and M. Hasna, "On relay assignment in network-coded cooperative systems," *IEEE Trans. Wireless Commun.,* vol. 10, pp. 868–876, Mar. 2011.

[14] X. Zhang, M. Hasna, and A. Ghrayeb, "Performance analysis of relay assignment schemes for cooperative networks with multiple source-destination pairs," *IEEE Trans. Wireless Commun.,* accepted.

[15] J. Huang, Z. Han, M. Chiang, and H. V. Poor, "Auction-based resource allocation for cooperative communications," *IEEE J. Sel. Areas Commun.,* vol. 26, pp. 1226–1237, Sep. 2008.

[16] J. Cai, X. Shen, J. W. Mark, and A. S. Alfa, "Semi-distributed user relaying algorithm for amplify-and-forward wireless relay networks," *IEEE Trans. Wireless Commun.,* vol. 7, pp. 1348–1357, Apr. 2008.

[17] H. Ochiai, P. Mitran, H. V. Poor, and V. Tarokh, "Collaborative beamforming for distributed wireless ad hoc sensor networks," *IEEE Trans. Signal Process.,* vol. 53, pp. 4110–4124, Nov. 2005.

[18] M. Haenggi, "On distances in uniformly random networks," *IEEE Trans. Inf. Theory,* vol. 51, pp. 3584–3586, Oct. 2005.

[19] K. Zarifi, A. Ghrayeb, and S. Affes, "Distributed beamforming for wireless sensor networks with improved graph connectivity and energy efficiency," *IEEE Trans. Signal Process.,* vol. 58, pp. 1904–1921, Mar. 2010.

[20] Y. Fan and J. Thompson, "MIMO configurations for relay channels: theory and practice," *IEEE Trans. Wireless Commun.,* vol. 6, pp. 1774–1786, May 2007.

[21] V. I. Morgenshtern and H. Bölcskei, "Crystallizations in large wireless networks," *IEEE Trans. Inf. Theory,* vol. 53, pp. 3319–3349, Oct. 2007.

[22] A. Blestas, A. Khisti, D. P. Reed, and A. Lippman, "A simple cooperative diversity method based on network path selection," *IEEE J. Sel. Areas Commun.,* vol. 24, pp. 659–672, Mar. 2006.

[23] W. Ye, J. Heidemann, and D. Estrin, "Medium access control with coordinated adaptive sleeping for wireless sensor networks," *IEEE/ACM Trans. Netw.,* vol. 12, pp. 493–506, June 2004.

[24] C. Bettstetter, "On the connectivity of ad hoc networks," *Comput. J.,* vol. 47, pp. 432–447, July 2004.

[25] Wireless Medium Access Control (MAC) and Physical Layer (PHY) Specifications for Low-Rate Wireless Personal Area Networks (LRW-PANs), IEEE Std. 802.15.4, 2003.

[26] ASH Transceiver TR3000 Data Sheet. Available: http://www.rfm.com/

Farrokh Etezadi received the B.Sc. degree in Electrical Engineering from the University of Tehran, Tehran, Iran, and the M.Sc. degree in Electrical and Computer Engineering from Concordia University, Montreal, Quebec, Canada, in 2007 and 2010, respectively. From January 2010 to August 2010, he was a Research Assistant in Concordia University when he worked on energy-efficient strategies for cooperative communication. In September 2010, he assumed his current position as a Research Assistant at Signals Multimedia and Security Laboratory in University of Toronto while pursuing his Ph.D. degree in Electrical Engineering. His research interests include information theory, multimedia communication and wireless communication. Mr. Etezadi has received a number of scholarships, including Concordia Graduate Scholarship, the Edward S. Rogers, Sr. Graduate Scholarship and the Ontario Graduate Scholarship.

Keyvan Zarifi (S'04, M'08) received his Ph.D. degree (with the highest honors) in Electrical and Computer Engineering from Darmstadt University of Technology, Darmstadt, Germany, in 2007.

Dr. Zarifi has held research appointments in the Department of Communication Systems, University of Duisburg–Essen, Duisburg, Germany, in the Department of Electrical and Computer Engineering, McMaster University, Hamilton, Ontario, Canada, and in École supérieure d'électricité (Supélec), Gif-sur-Yvette, France. From September 2007 to May 2011, he has been jointly with Institut National de la Recherche Scientifique-Énergie, Matériaux, et Télécommunications (INRS-EMT), Université du Québec, and Concordia University, Montreal, Quebec, Canada, as a Post-doctoral Fellow. He is now a Senior Engineer in Huawei Technologies, Kanata, ON, Canada. His research interests include statistical signal processing, wireless sensor networks, MIMO and cooperative communications, and blind estimation and detection techniques. In 2008, Dr. Zarifi has received Postdoctoral Fellowship from the Natural Sciences and Engineering Research Council of Canada (NSERC).

Ali Ghrayeb (S'97, M'00, SM'06) (SŠ97-MŠ00-SMŠ06) received the Ph.D. degree in electrical engineering from the University of Arizona, Tucson, USA in 2000. He is currently a Professor with the Department of Electrical and Computer Engineering, Concordia University,Montreal, QC, Canada.

He is a co-recipient of the IEEE Globecom 2010 Best Paper Award. He holds a Concordia University Research Chair in Wireless Communications. He is the coauthor of the book Coding for MIMO Communication Systems (Wiley, 2008). His research interests include wireless and mobile communications, error correcting coding, MIMO systems, wireless cooperative networks, and cognitive radio systems.

Dr. Ghrayeb has instructed/co-instructed technical tutorials at several major IEEE conferences. He co-chaired the IEEE Globecom 2011 Communications Theory Symposium. He serves as an Editor of the IEEE TRANSACTIONS ON COMMUNICATIONS, IEEE TRANSACTIONS ON WIRELESS COMMUNICATIONS and the *Physical Communications Journal*. He served as an Editor of IEEE TRANSACTIONS ON SIGNAL PROCESSING, an Associate Editor of IEEE TRANSACTIONS ON VEHICULAR TECHNOLOGY and the *Wiley Wireless Communications and Mobile Computing Journal*.

Sofiène Affes (S'94, M'95, SM'04) received the Diplôme d'Ingénieur in telecommunications in 1992, and the Ph.D. degree with honors in signal processing in 1995, both from the École Nationale Supérieure des Télécommunications (ENST), Paris, France.

He has been since with INRS-EMT, University of Quebec, Montreal, Canada, as a Research Associate from 1995 till 1997, as an Assistant Professor till 2000, then as an Associate Professor till 2009. Currently he is a Full Professor in the Wireless Communications Group. His research interests are in wireless communications, statistical signal and array processing, adaptive space-time processing and MIMO. From 1998 to 2002 he has been leading the radio design and signal processing activities of the Bell/Nortel/NSERC Industrial Research Chair in Personal Communications at INRS-EMT, Montreal, Canada. Since 2004, he has been actively involved in major projects in wireless of PROMPT (Partnerships for Research on Microelectronics, Photonics and Telecommunications).

Professor Affes was the co-recipient of the 2002 Prize for Research Excellence of INRS. He currently holds a Canada Research Chair in Wireless Communications and a Discovery Accelerator Supplement Award from NSERC (Natural Sciences and Engineering Research Council of Canada). In 2006, Professor Affes served as a General Co-Chair of the IEEE VTC'2006-Fall conference, Montreal, Canada. In 2008, he received from the IEEE Vehicular Technology Society the IEEE VTC Chair Recognition Award for exemplary contributions to the success of IEEE VTC. He currently acts as a member of the Editorial Board of the IEEE TRANSACTIONS ON SIGNAL PROCESSING, the IEEE TRANSACTIONS ON WIRELESS COMMUNICATIONS, and the *Wiley Journal on Wireless Communications & Mobile Computing*.